Heliyon 10 (2024) e28768

Contents lists available at ScienceDirect

Heliyon

journal homepage: www.cell.com/heliyon

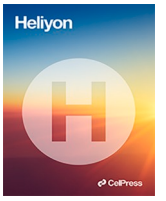

Research article

Cardiac magnetic resonance feature tracking derived left atrial strain in the diagnosis of patients with constrictive pericarditis and restrictive cardiomyopathy

Kairui Bo [a], Yichen Zhao [b], Xuelian Gao [a], Yanchun Chen [a], Yue Ren [a], Yifeng Gao [a], Zhen Zhou [a], Hui Wang [a,*], Lei Xu [a,**]

[a] Department of Radiology, Beijing Anzhen Hospital, Capital Medical University, Beijing, 100029, China
[b] Department of Cardiac Surgery, Beijing Anzhen Hospital, Capital Medical University, Beijing, 100029, China

ARTICLE INFO

Keywords:
Constrictive pericarditis
Restrictive cardiomyopathy
Left atrium
Myocardial strain

ABSTRACT

Objective: To explore the diagnostic value of cardiac magnetic resonance feature tracking (CMR-FT) divided left atrial (LA) strain in differentiating constrictive pericarditis (CP) and restrictive cardiomyopathy (RCM).

Methods: Patients with CP (n = 40) and RCM (n = 40), and another 40 normal control group were retrospectively enrolled over a period of 8 years at a tertiary cardiac centre. Left ventricular (LV) and biatrial strain and strain rate (SR) were measured. Atrial strain was used to differentiate between patients with CP and RCM. Then, patients were grouped according to their left ventricular ejection fraction (LVEF), either ≥50% or < 50%. A deeper analysis was done to evaluate the diagnostic value of atrial strain in these subgroups. Receiver operating characteristic curves (ROC) were used to assess the accuracy of myocardial strain based on CMR FT for the differential diagnosis of CP and RCM.

Results: LV and LA strain and SR were significantly lower in patients with CP and RCM than those in the normal controls ($P < 0.05$). LA strain and SR were significantly lower in the RCM group than in the CP group ($P < 0.05$). In patients with either LVEF≥50% or < 50%, LA strain were lower in the RCM group than in the CP group ($P < 0.05$). ROC analysis showed that LA stored strain (LA-*es*) had a good differential diagnostic value for CP and RCM, with an area under the curve (AUC) of 0.811 and an optimal cutoff value of 6.98%, above this value it tends to develop CP. Further, an excellent differential diagnostic value was found in patients with LVEF < 50%, with an AUC of 0.955.

Conclusion: LA strain analysis obtained by CMR-FT provides good differential diagnostic value for distinguishing CP from RCM, especially in patients with LVEF < 50%.

* Corresponding author. Department of Radiology, Beijing Anzhen Hospital, Capital Medical University, Beijing, No. 2 Anzhen Rd, Chaoyang District, Beijing, 100029, China.

** Corresponding author. Department of Radiology, Beijing Anzhen Hospital, Capital Medical University, Beijing, No. 2 Anzhen Rd, Chaoyang District, Beijing, 100029, China.

E-mail addresses: bo20200@126.com (K. Bo), zhaoyichen_2011@hotmail.com (Y. Zhao), gaoxuelian0822@163.com (X. Gao), 591410217@qq.com (Y. Chen), ry11182022@163.com (Y. Ren), 122019000788@ccmu.edu.cn (Y. Gao), alexzhou@ccmu.edu.cn (Z. Zhou), hugeren@126.com (H. Wang), leixu2001@hotmail.com (L. Xu).

https://doi.org/10.1016/j.heliyon.2024.e28768
Received 28 February 2024; Received in revised form 22 March 2024; Accepted 24 March 2024
Available online 28 March 2024

1. Introduction

Constrictive pericarditis (CP) [1,2]is manifested as pericardial thickening, adhesion and calcification caused by chronic inflammatory lesions of the pericardium due to various causes. CP limits the diastolic and systolic function of the heart with resultant a series of symptoms of circulatory disorders. Restrictive cardiomyopathy (RCM) is characterized by the coexistence of persistent restrictive pathophysiology, commonly with atrial dilatation, and nondilated ventricles, regardless of ventricular wall thickness and systolic function [3]. CP is mimic to RCM in pathophysiology and clinical manifestations, which make it presents challenges in the differential diagnosis. Despite relatively high mortality associated with open repair, most CP can be cured by pericardiectomy if treated promptly with good prognosis; while RCM has no specific prevention and treatment, and has a poor prognosis and eventually requires heart transplantation, so correct differential diagnosis is essential [4].

Differentiating RCM from CP by transcatheter endocardial biopsy or exploratory thoracotomy undoubtedly has certain limitations [5]. Pericardial thickening and "interventricular septal sway" phenomenon with respiratory motion observed by echocardiography or chest CT often suggest CP [6], however, if pericardial thickening and "interventricular septal sway" phenomenon are atypical, it is difficult to differentiate these two conditions [7]. In recent years, it has been reported that patients with RCM and CP usually present with left atrial enlargement and impaired function, thus, assessment of left atrial dysfunction is considered helpful to differentiate the two scenarios [8,9].

However, increased atrial volume does not explain changes in the atrial function throughout the cardiac cycle. Cardiac magnetic resonance-feature tracking (CMR-FT), as a new technique that can quantitatively analyze global and regional myocardial mechanical changes in heart allows quantitatively measurement of atrial strain changes throughout the cardiac cycle to assess atrial reservoir, conduit, and booster function [10,11]. Previous studies have confirmed that CMR-FT is useful in differentiating RCM from CP by assessing the left ventricular global longitudinal strain (LV-GLS) [12,13]. However, no study has investigated whether the clinical value of CMR-FT atrial strain in differentiating CP from RCM is better than ventricular strain, and this study aimed to address this research gap by applying CMR-FT to quantitatively evaluate biatrial and left ventricular strain in patients with CP and RCM, and explored its diagnostic value in differentiating these two conditions.

2. Methods

1. **Subjects:** This retrospective study involved analysis of patients who were diagnosed with CP and RCM from January 2015 to January 2023 in Beijing Anzhen Hospital. CMR and echocardiography were performed in all participants. The patients with no abnormality confirmed by ECG and echocardiography and basically normal CMR examination in the same period were selected as the control group. Patients were divided into subgroups with left ventricular ejection fraction (LVEF) $\geq$ 50% and $<$50%.

CP group inclusion criteria [13,14]: (1) confirmed by pericardiectomy surgery; (2) those who did not undergo pericardiectomy surgery met echocardiographic or chest CT confirmation of pericardial thickness $\geq$4 mm, and/or echocardiographic and CMR suggested the presence of interventricular septum swing with respiration. Exclusion criteria: Definite diagnosis of cardiomyopathy by surgery or myocardial biopsy.

RCM group inclusion criteria [3,15]: (1) CMR late gadolinium enhancement (LGE) confirmed endomyocardial infiltration involvement, while echocardiography or CMR met all of the following criteria: interventricular septum thickness $\geq$12 mm; left ventricular filling restriction, left and right atrial enlargement. (2) Amyloidosis on cardiac or other tissue biopsy. Exclusion criteria: Definite diagnosis of pericardial disease and malignant arrhythmia, valvular disease, myocardial infarction, hypertension and other causes of myocardial hypertrophy and dysfunction.

This study was approved by the Ethics Committee of Beijing Anzhen Hospital, Capital Medical University (Approval No. 2006003X). Written informed consent was waived by the Institutional Review Board due to the respective nature of the study.

2. **CMR scanning protocol:** All patients underwent CMR scanning using a 32-channel phased array coil under respiratory navigation and electrocardiographic gating. The scan was performed on 3.0T CMR scanners (Achieva, Philips, Netherlands, Holland). Standardized imaging protocols included Steady state free precession (SSFP) breath-hold cine images and LGE [16]. Contiguous short-axis slices (8 mm thickness, no gap) were used to cover the entire left ventricle from the annulus of AV valves to the apex, with 25 phases per cardiac cycle. Long-axis planes (2-chamber, 4-chamber, 3-chamber views) were acquired with 5 mm slice thickness and no gap. LGE images were obtained using a prospectively EKG-gated gradient echo sequence after intravenous gadolinium infusion. Imaging parameters of LGE included repetition time/echo time of 4.1/1.6 ms, flip angle of 20°, and image matrix of 256 $\times$ 130.
3. **Left ventricular and biatrial strain analysis:** Cardiac function analysis was performed using the Cvi42 (5.2.0, Circle, Canada). Short 3D module to obtain left ventricular function parameters using ventricular short-axis cardiac sequences to semi-automatically identify and delineate epicardial and endocardial boundaries at end-systole and diastole. The ventricular chamber consisted of papillary muscle and chordae tendineae. Left atrial volume and ejection fraction mean left atrial volume and atrial ejection fraction were measured on 2- and 4-chamber biplane cine images. Right atrial volume and ejection fraction were measured on 4-chamber cine images. Left ventricular and biatrial function was analyzed using Cvi42 commercial software.

Myocardial strain was analyzed using the CVI42 tissue tracking module. End-diastolic cine images were selected, and the endocardium and epicardium delineating short-axis and long-axis cine images were automatically identified by the software, and the

inaccuracy was identified and corrected by experts with >10 years of experience in cardiovascular imaging diagnosis, and LV-GLS were automatically generated after operation. The left atrial strain parameters were analyzed with 2-chamber and 4-chamber cine images, and the right atrial strain parameters were analyzed with 4-chamber cine images. The endocardial and epicardial boundaries of the atrium (except veins and appendages) were manually traced at the largest and smallest central atrial volume on 2- and 4-chamber cine images, respectively, delineated by a cardiovascular imaging specialist with more than 10 years of experience using a point-matching method [17].

Fig. 1 shows the delineation method of the atrial boundaries. The endocardial and epicardial boundaries then propagate automatically to all phases during the cardiac cycle (25 frames/cardiac cycle) to obtain atrial reservoir(εs), conduit(εe), and booster(εa) strain and Strain Rate (SR). In cases where feature tracking was not ideal, endocardial boundaries were manually adjusted. The epicardial and endocardial contours of each slice were manually delineated on LGE short-axis images, and a region of interest of the normal myocardium was selected, and the software automatically showed regions with signal intensities 5 standard deviations higher than those of the normal myocardium, defined them as regions with LGE and automatically obtained the mass of LGE (in grams) as a percentage of the total mass of the left ventricular myocardium.

4 Reproducibility analysis

Forty patients were randomly selected to investigate intraobserver and interobserver agreement for biatrial strain, including εs, εe, and εa strain. Interobserver agreement: atrial strain was independently measured in 40 patients by a second radiologist experienced in CMR diagnosis who was blinded to the first observer's results. Intraobserver agreement: atrial strain measurement was repeated in these 40 patients after an interval of 1 month by the same observer.

5. **Statistical analysis:** Statistical analysis was performed using SPSS 25.0 (SPSS, Inc, Chicago, IL, USA). For continuous variables conforming to normal distribution, data were presented as mean ± standard deviation (SD); data with skewed distribution were presented as median and interquartile range (IQR). Categorical variables were presented as percentages and frequencies. Differences in clinical and CMR parameters were compared using an analysis of variance (ANOVA test) for continuous variables that followed a normal distribution, and Kruskal-Wallis test for continuous variables with unequal variance. For continuous variables with non-normal distribution, Kruskal-Wallis test was used for inter-compartmental comparison. Differences between groups were

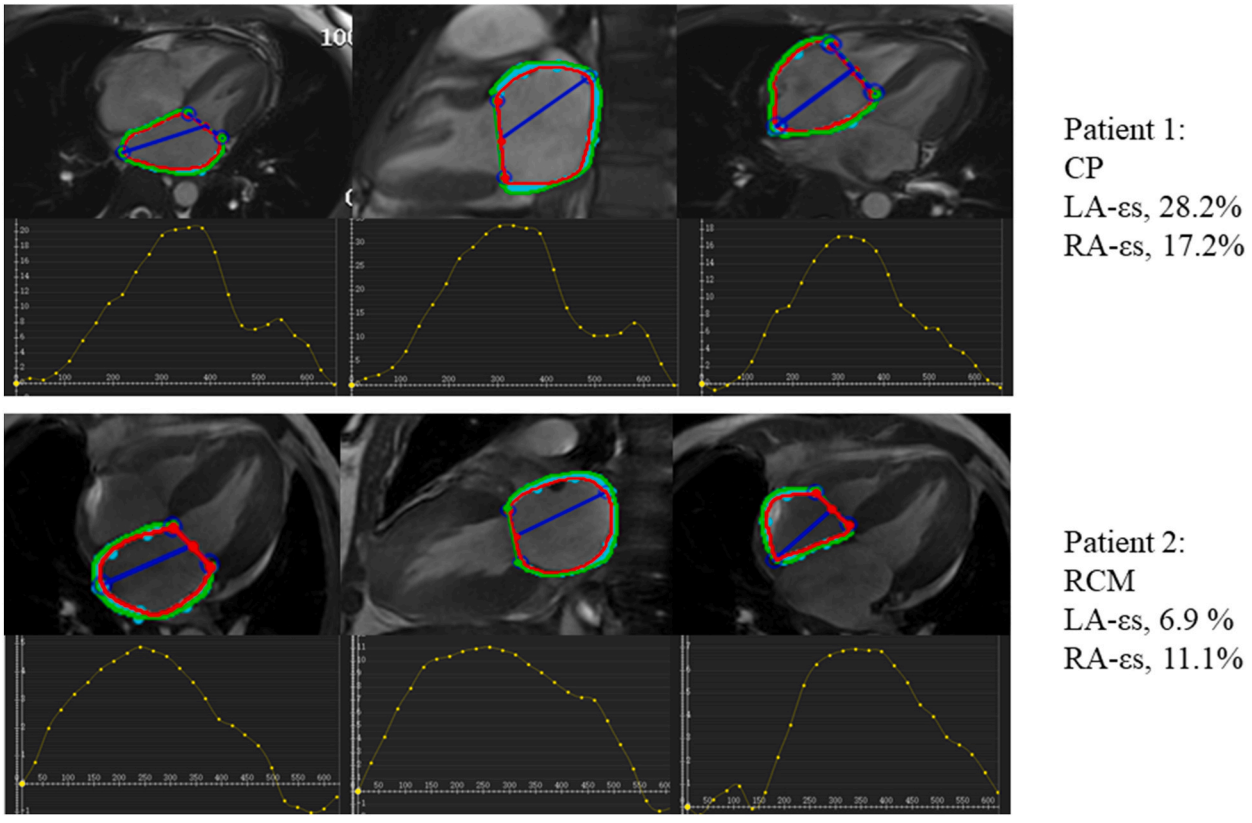

Fig. 1. Showing the delineation of left atrial and right atrial strain contours in patients with constrictive pericarditis (CP) and restrictive cardiomyopathy (RCM) using CMR left ventricular two-chamber and four-chamber cardiac sequences.

compared using the Chi-square test for dichotomous variables. Receiver operating characteristic (ROC) curves were used to evaluate the value of each measurement for the differential diagnosis between CP and RCM, and the optimal cutoff value was selected. Interobserver and intraobserver agreement for ventricular strain parameters were assessed using intraclass correlation coefficients (ICCs). ICC <0.4 indicated poor agreement, and ICC >0.75 signified good agreement. $P < 0.05$ was considered statistically significant.

3. Results

The general clinical data of the three groups are shown in Table 1: A total of 40 CP patients, aged 48.23 ± 17.73 years, and 40 RCM patients, aged 54.68 ± 12.44 years, were enrolled in this study. At the same time, 40 normal controls were enrolled. Among the patients in the CP group, 14 (35%) were confirmed by pericardiectomy surgery, 23 (83%) by echocardiography or CMR with pericardial thickness ≥4 mm, and 25 (43%) by both echocardiography and CMR showed the presence of interventricular septum swinging with respiration. Among the patients in the RCM group, 39 (97.5%) had myocardial infiltration involvement confirmed by LGE imaging, 2 (5%) had myocardial amyloidosis confirmed by myocardial biopsy, and 10 (25%) had myocardial amyloidosis suggested by extracardiac biopsy. There were no statistically significant differences in age, gender composition, or heart rate between patients in the CP group and those in the RCM group. Echocardiography and CMR showed that LVEF was significantly lower in CP and RCM groups than in the normal controls ($P < 0.05$), but there was no significant difference between these two diseased groups ($P > 0.05$). CMR showed that left ventricular myocardial mass was greater in patients in the RCM group than in the CP group ($P < 0.05$).

CMR-FT analysis showed that LV-GLS were lower in CP and RCM groups than in normal controls ($P < 0.05$). εs, εe, εa and SR in left atrium (LA) and right atrium (RA) were lower than those in normal controls ($P < 0.05$). LV-GLS, LA-εs, LA-εe and LA-εa and LA-SR in the RCM group were significantly lower than those in the CP group ($P < 0.05$ for all), while right atrial strain and strain rate were not significantly different between the two groups ($P > 0.05$), as detailed in Table 2 and Fig. 2. ROC curve analysis showed that LA-εs and LA-εe had good diagnostic value for differentiating CP from RCM (AUC = 0.811, 0.807, respectively), as shown in Fig. 3a. The optimal cutoff value of LA-εs was 6.98, which tended to be RCM below 6.98, and vice versa tended to be CP, with a sensitivity of 90% and a specificity of 63%.LV-GLS, LA-εs, LA-εe, and LA-εa were lower in the RCM group than in the CP group ($P < 0.05$) in the patients with either LVEF ≥50% or < 50%, as shown in Table 3 and Fig. 4. ROC curve analysis showed that LA-εs had a good diagnostic value for differentiating CP from RCM in the subgroup with LVEF≥50%, with an AUC of 0.769, and an excellent value in patients with LVEF < 50%, with an AUC of 0.955, as shown in Fig. 3BCE Meantime, the AUC of LV-GLS in the patients with LVEF≥50% and < 50% were 0.717 and 0.758, respectively(Fig. 3).

Table 1
Baseline characteristics of constrictive pericarditis, restrictive cardiomyopathy and control groups.

Basic characteristics	CP (n = 40)	RCM (n = 40)	Control (n = 40)	P value
Age, years	48.23 ± 17.73	54.68 ± 12.44	48.80 ± 10.15	0.073
Male sex, (%)	24(60.00)	30(75.00)	20(50.00)	0.074
Height, cm	168.55 ± 7.91	166.70 ± 8.50	167.30 ± 6.55	0.551
Weight, kg	68.30 ± 12.01	68.86 ± 13.77	69.99 ± 11.20	0.825
BMI, kg/m2	23.98 ± 3.67	24.67 ± 3.89	24.94 ± 3.33	0.476
Heart rate, bpm	81.50(80.83–92.40)	80(74.55–84.11)	68.33(62.60–72.57)[a.b]	**<0.001**
Atrial fibrillation, n (%)	14(35.00)	10(25.00)	0(0.00)[a.b]	**<0.001**
Hypertension, n (%)	4(10.00)	10(25.00)	6(15.00)	0.189
Hyperlipidemia, n (%)	2(5.00)	9(22.50)	4(10.00)	0.053
Diabetes mellitus, n (%)	2(5.00)	3(7.50)	5(12.50)	0.606
Familial history of CAD, n (%)	3(7.50)	8(20.00)	2(5.00)	0.071
Echocardiogram				
LVEF, %	59(54,65.25)	58(54–65.25)	63.50(63.50–64.63)[a.b]	**<0.001**
LVEDD, mm	41.95 ± 6.62	45.60 ± 5.16[c]	46.6 ± 3.78[a.b]	**<0.001**
LVEDS, mm	27.99 ± 5.30	31.03 ± 4.25[c]	28.47 ± 3.49[a]	**0.005**
E wave, m/s	88.53 ± 23.86	94.25 ± 33.96	85.15 ± 16.89	0.295
A wave, m/s	55.70 ± 20.56	67.98 ± 27.71[c]	65.38 ± 14.45[b]	**0.031**
E/A wave	1.78 ± 0.86	1.65 ± 1.04	1.35 ± 0.34	0.056
CMR				
LVEF, %	51.30 ± 11.54	48.22 ± 12.19	61.48 ± 5.65[a.b]	**<0.001**
LVEDV, mL	96.44 ± 34.46	112.43 ± 34.71[c]	119.32 ± 24.78[b]	**0.005**
LVESV, mL	47.16 ± 22.93	57.92 ± 26.74[c]	46.29 ± 12.69[a.b]	**0.031**
LVMASS, g	91.60(54.11,85.52)	127.20(91.58,185.50)[c]	78.85(59.73,97.41)[b]	**<0.001**
LGE of myocardium, %	17.50	97.50	…	…

CP, constrictive pericarditis; RCM, restrictive cardiomyopathy; BMI, body mass index; LVEF, left ventricular ejection fraction; EDD, end-diastolic diameter; ESD, end systolic diameter.
CMR, Cardiac magnetic resonance; EDV, left ventricular end-diastolic volume; ESV, left ventricular end-systolic volume; LVMASS, left ventricular mass; LGE, Delayed gadolinium enhancement.
[a] P<0.05 Control vs CP by Mann–Whitney tests.
[b] P < 0.05 Control vs RCM by Mann-Whitney tests.
[c] P < 0.05 RCM vs CP by Mann-Whitney tests.

Table 2
CMR-FT-derived assessment of left and right atrial and left ventricular strain.

Characteristics of CMR	CP (n = 40)	RCM (n = 40)	Control (n = 40)	P value
LVGLS, %	11.60(8.05–14.20)	7.70(5.40–11.48)[c]	18.20(16.03–19.30)[a,b]	<0.001
LAEF, %	36.82(20.26–44.84)	25.55(18.23–36.67)	57.42 (53.24–63.02)[a,b]	<0.001
LAVmax,mL	82.54(58.03–116.16)	92.21(61.54–131.35)	55.04 (40.32–67.78)[a,b]	<0.001
LAVmin,mL	54.95(31.42–76.75)	68.04(41.45–98.72)	22.19 (17.47–26.62)[a,b]	<0.001
LA-εs, %	14.25(9.41–21.38)	5.68(4.08–10.39)[c]	34.63 (29.38–16.53)[a,b]	<0.001
LA-εe, %	7.95(5.25–12.66)	3.48(1.96–5.76)[c]	20.05 (16.96–23.44)[a,b]	<0.001
LA-εa, %	5.55(3.56–9.09)	2.68(1.68–4.75)[c]	14.13 (12.38–16.53)[a,b]	<0.001
LA-SRs, sec^{-1}	1.00(0.61–1.55)	0.60(0.36–0.89)[c]	1.75 (1.51–2.19)[a,b]	<0.001
LA-SRe, sec^{-1}	1.10(0.66–1.96)	0.45(0.35–0.68)[c]	2.13 (1.86–2.60)[a,b]	<0.001
LA-SRa, sec^{-1}	0.88(0.48–1.40)	0.43(0.31–0.59)[c]	2.00 (1.60–2.25)[a,b]	<0.001
RAEF, %	28.80(19.58–39.88)	28.88(16.21–41.53)	52.94 (48.97–57.92)[a,b]	<0.001
RAVmax, ml	66.04(47.49–90.09)	57.94(35.46–95.65)	49.07 (34.45–66.02)[a,b]	0.006
RAVmin, ml	40.55(27.66–62.11)	40.56(23.36–75.29)	23.78 (16.56–28.84)[a,b]	<0.001
RA-εs, %	7.90(5.00–19.78)	8.90(4.60–14.25)	35.10 (29.98–39.60)[a,b]	<0.001
RA-εe, %	4.25(1.98–9.40)	5.80(7.60–8.91)	21.05 (16.88–27.43)[a,b]	<0.001
RA-εa, %	4.10(2.50–10.45)	5.48(2.38–10.11)	12.50 (10.58–15.18)[a,b]	<0.001
RA-SRs, sec^{-1}	0.70(0.50–1.50)	0.75(0.50–1.10)	1.95 (1.50–2.40)[a,b]	<0.001
RA-SRe, sec^{-1}	0.50(0.40–1.40)	0.60(0.30–0.80)	1.90 (1.53–2.58)[a,b]	<0.001
RA-SRa, sec^{-1}	0.75(0.33–1.43)	0.70(0.33–1.00)	1.75 (1.40–2.40)[a,b]	<0.001

CMR, Cardiac magnetic resonance; CP, constrictive pericarditis; RCM, restrictive cardi-omyopathy; LVGLS, left ventricular global longitudinal strain; LAEF, Left atrial ejection fraction; LAVmax, Maximum left atrial volume; LAVmin, Minimum left atrial volume; εs, reservoir strain; εe, conduit strain; εa, booster strain; SRs, peak positive strain rate; SRe, peak early negative strain rate; SRa, peak late negative strain rate; RAEF, Right atrial ejection fraction; RAVmax, Maximum right atrial volume; RAVmin,Minimum right atrial volume.

[a] P<0.05 Control vs CP by Mann–Whitney tests.

[b] P < 0.05 Control vs RCM by Mann-Whitney tests.

[c] P < 0.05 RCM vs CP by Mann-Whitney tests.

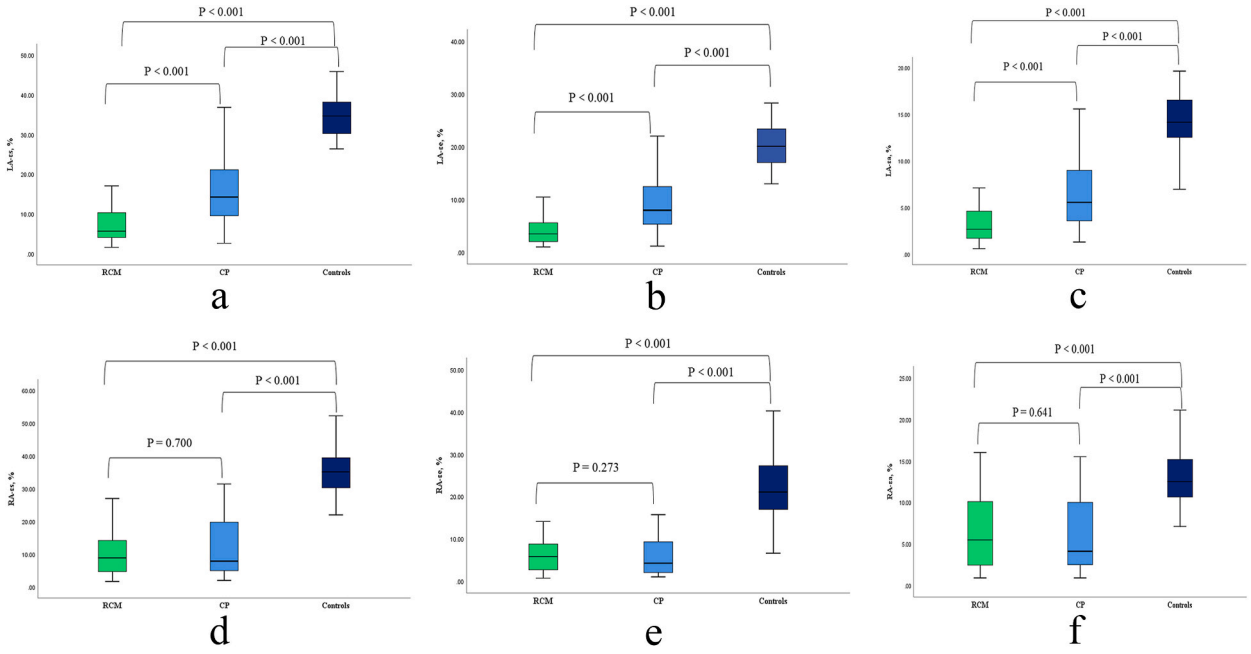

Fig. 2. Box plot of left and right atrial strain in constrictive pericarditis (CP), restrictive cardiomyopathy (RCM), and controls. a: LA-εs, Left atrial reservoir strain; b: LA-εe, Left atrial conduit strain; c: LA-εa, Left atrial booster strain d: RA-εs, Reft atrial reservoir strain; e: RA-εe, Reft atrial conduit strain; f: RA-εa, Reft atrial booster strain.

Biatrial strain had good intraobserver and interobserver repeatability. The interobserver ICCs of LA-εs, LA-εe, LA-εa RA-εs, RA-εe, RA-εa were 0.981, 0.960, 0.865, 0.954, 0.952 and 0.857 respectively, and the intraobserver ICCs were 0.994, 0.986, 0.951, 0.984,0.983and 0.947 respectively, with p values < 0.05.

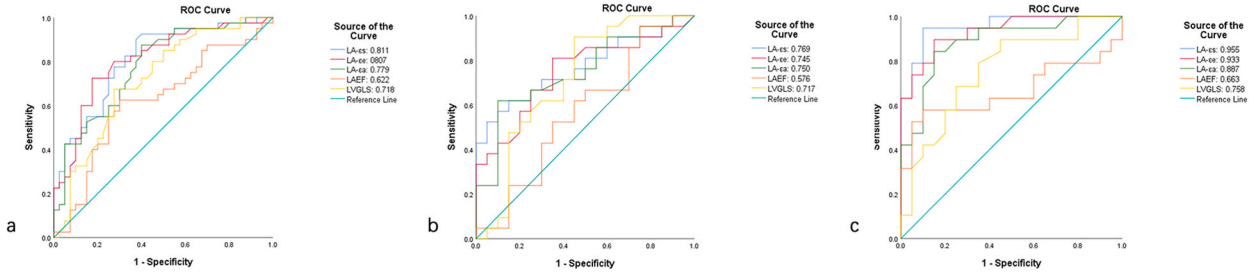

Fig. 3. Box plot of left atrial and left ventricular strain in constrictive pericarditis (CP), restrictive cardiomyopathy (RCM) in two subgroups of left ventricular ejection fraction (LVEF) ≥ 50% and <50%. a–d: LVEF≥ 50%: LVGLS, left ventricular global longitudinal strain; LA-εs, Left atrial reservoir strain; LA-εe, Left atrial conduit strain; LA-εa, Left atrial booster strain. e–h: LVEF <50%: LVGLS, left ventricular global longitudinal strain; LA-εs, Left atrial reservoir strain; LA-εe, Left atrial conduit strain; LA-εa, Left atrial booster strain.

Table 3
CMR-FT-derived assessment of left atrial and left ventricular strain in subgroup analyses.

CMR-LVEF≥50%	CP (n = 21)	RCM (n = 20)	Control (n = 40)	P value
LVEF,%	59.96 ± 5.55	58.63 ± 6.91	61.48 ± 5.65[a,b]	0.208
LVGLS, %	12.90(11.00–14.60)	19.70(7.28–12.48)[c]	18.20(16.03–19.30)[a,b]	**<0.001**
LAEF, %	40.71(23.30–50.95)	33.41(18.72–49.09)	57.42 (53.24–63.02)[a,b]	**<0.001**
LA-εs, %	20.25(11.00–28.08)	9.50(4.81–15.41)[c]	34.63 (29.38–16.53)[a,b]	**<0.001**
LA-εe, %	9.95(6.60–16.00)	5.10(2.79–8.61)[c]	20.05 (16.96–23.44)[a,b]	**<0.001**
LA-εa, %	7.70(4.35–10.70)	4.53(2.14–6.66)[c]	14.13 (12.38–16.53)[a,b]	**<0.001**
RAEF, %	36.19(25.38–49.91)	38.20(13.77–44.93)	52.94 (48.97–57.92)[a,b]	**<0.001**
RA-εs, %	19.60(7.00–22.15)	11.65(16.33–5.03)	35.10 (29.98–39.60)[a,b]	**<0.001**
RA-εe, %	7.40(2.45–10.20)	7.05(2.91–9.76)	21.05 (16.88–27.43)[a,b]	**<0.001**
RA-εa, %	8.40(3.15–13.00)	5.90(2.45–10.86)	12.50 (10.58–15.18)[a,b]	**<0.001**
CMR-LVEF < 50%	CP (n = 19)	RCM (n = 20)	Control (n = 40)	P value
LVEF,%	41.74 ± 8.38	37.82 ± 5.40	61.48 ± 5.65[a,b]	**<0.001**
LVGLS, %	8.00(7.00–11.90)	6.05(4.93–7.75)[c]	18.20(16.03–19.30)[a,b]	**<0.001**
LAEF, %	34.54(18.53–41.62)	21.63(17.99–26.96)	57.42 (53.24–63.02)[a,b]	**<0.001**
LA-εs, %	10.45(8.50–17.70)	4.60(3.55–6.01)[c]	34.63 (29.38–16.53)[a,b]	**<0.001**
LA-εe, %	7.55(4.35–9.85)	2.53(1.75–3.49)[c]	20.05 (16.96–23.44)[a,b]	**<0.001**
LA-εa, %	3.90(3.30–6.65)	2.02(1.44–2.94)[c]	14.13 (12.38–16.53)[a,b]	**<0.001**
RAEF, %	23.32(15.08–34.68)	26.08(16.39–36.59)	52.94 (48.97–57.92)[a,b]	**<0.001**
RA-εs, %	6.10(4.00–8.20)	7.45(4.60–13.05)	35.10 (29.98–39.60)[a,b]	**<0.001**
RA-εe, %	3.40(1.50–4.30)	4.60(2.43–7.58)	21.05 (16.88–27.43)[a,b]	**<0.001**
RA-εa, %	2.80(1.90–4.30)	4.38(2.38–9.70)	12.50 (10.58–15.18)[a,b]	**<0.001**

CMR, Cardiac magnetic resonance; CP, constrictive pericarditis; RCM, restrictive cardiomyopathy; LVEF, left ventricular ejection fraction; LVGLS, left ventricular global longitudinal strain; LAEF, Left atrial ejection fraction; εs, reservoir strain; εe, conduit strain; εa, booster strain; RAEF, Right atrial ejection fraction.

[a] P<0.05 Control vs CP by Mann–Whitney tests.

[b] P < 0.05 Control vs RCM by Mann-Whitney tests.

[c] P < 0.05 RCM vs CP by Mann-Whitney tests.

4. Discussion

This study showed that εs, εe, εa, and SR were generally decreased in the left and right atria strain analysis of patients with CP and RCM compared with the controls. This suggests that atrial strain can predict the cardiac function changes in patients with CP and RMC at an early stage. Quantitative analysis of the strain in the left atrium rather than the right atrium is more sensitive in quantificationally differentiating CP from RCM. LA-εs showed superior differential diagnostic value over LVGLS in both subgroups with preserved LVEF and reduced LVEF.

Some studies have demonstrated that left atrial function plays an important role in the diagnosis and prognostic evaluation of cardiomyopathy [18–20]. Atrial strain reflects cardiac dysfunction earlier than atrial volume and LVEF [21]. Also, it has been shown that left atrial strain is associated with left atrial structural remodeling and atrial wall fibrosis [22]. CP and RCM are known as causes of increased left ventricular filling pressure, and increased atrial afterload due to increased ventricular filling pressure is considered to be the main mechanism of atrial dysfunction in both, however, the characteristics of atrial strain in patients with CP and RCM remain unclear. Atrial strain and SR evaluated by CMR-FT are the two reliable parameters that have been reported as a feasible and reproducible method for assessing myocardial function [17,23,24]. To our knowledge, this is the first study to report the diagnostic value of atrial strain analysis in patients with CP and RCM using CMR-FT.

In patients with CP, due to pericardial restriction of the left ventricle, left atrial pressure increases to maintain adequate left ventricular filling pressure, while increased atrial wall tension leads to atrial enlargement and myocardial stretching. The reduced

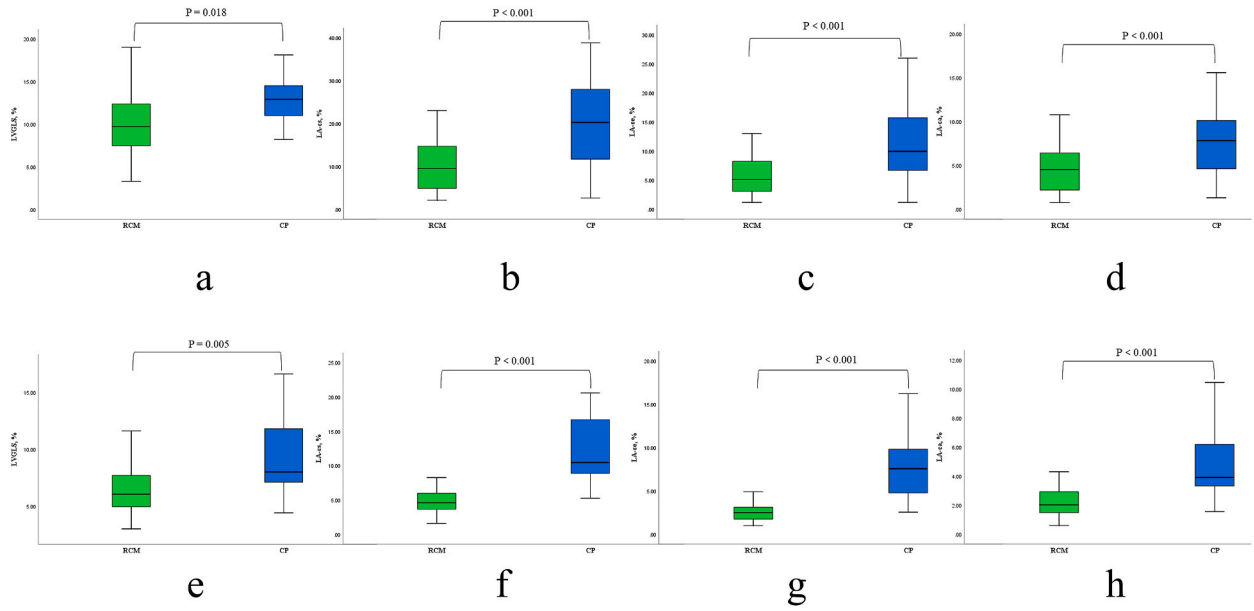

Fig. 4. a: Receiver operating characteristic curve of left atrial and left ventricular strain parameters in all patients. b: Receiver operating characteristic curve of left atrial and left ventricular strain parameters in LVEF≥50% patients. c: Receiver operating characteristic curve of left atrial and left ventricular strain parameters in LVEF < 50% patients.

atrial reservoir function, pericardial restriction of the left ventricle and secondary organic changes in the atrial myocardium may lead to reduced atrial conduit and booster function [8]. In patients with RCM, an increase in myocardial stiffness leads to a significant increase in ventricular pressure, which induces hemodynamic changes similar to CP. However, there are many factors causing RCM, such as endomyocardial fibrosis, cardiac amyloidosis (CA), glycogen reservoir disease, drug-induced or radiation-induced myocardial degeneration can lead to myocardial cell or myocardial cell interstitial infiltration fibroplasia, which leads to left ventricular diastolic dysfunction. In the case of common CA, previous results on CA autopsy patients showed that amyloidosis often involves the left and right atria, even in the absence of left ventricular involvement [25,26]. This atrial deposition of amyloid fibrin leads to abnormal atrial structure and function [27], which in severe cases can lead to electrocardio-mechanical dissociation, causing the LA to lose its pump function filling the left ventricle, and then thromboembolic events or even sudden death. The general decrease in atrial strain and SR in our patients with RCM also confirms these findings.

LA strain instead of RA strain showed a good diagnostic value in differentiating CP from RCM. This may be due to the following reasons: Pericardial contraction is characterized pathophysiologically by the restriction of outward expansion of the cardiac chambers, which is caused by the restriction of rigid, fixed pericardial volume. The oblique pericardial sinus lies posterior to the LA, so the posterior wall of the LA is actually separated from the pericardial space. Compared to RA, outward dilatation of the LA may be less restricted by rigid and fixed pericardium in patients with CP [28], which may result in less left atrial damage in patients with CP. In addition, the morphological changes of the right ventricle are also closely related to the site of pericardial thickening. When severe constriction occurs, tubular stenosis of the right ventricular cavity can also be considered as one of the characteristic features of CP. At this time, RA and superior and inferior vena cava are dilated, and the right atrial function is more severely damaged than the LA [29]. In patients with RCM, restrictive physiology caused by reduced myocardial compliance affects both ventricles, whereas the normally compliant pericardium allows significant dilation of both the left and right atria. At the same time, infiltration of atrial myocardium will further increase the stiffness of atrial myocardium and aggravate left and right atrial function impairment in patients with RCM [30,31]. These results suggest that the LA is a useful index for differentiating CP from RCM, and a cutoff value of LA-εs of 6.98% contributes to the quantitative diagnosis of both diseases. These findings are of clinical significance since substantial distinctions between CP and RCM are not easily achieved by extensive clinical and non-invasive testing.

In addition, previous studies [12,32] suggest that left ventricular GLS is decreased in RCM patients compared with CP patients, which may be due to the fact that RCM mainly leads to subendocardial myocardial fibrosis and reduced LV-GLS in damaged endomyocardial myocardium. Our study also confirmed the diagnostic value of GLS, with ROC analysis showing that left atrial strain was superior to LV-GLS in differentiating CP from RCM in both subgroups of LVEF ≥50% and <50%, suggesting a potential clinical diagnostic value advantage of LA strain. In particular, for patients with LVEF <50%, impaired ventricular function may reduce the efficacy of differential diagnosis of ventricular strain, and further analysis of left atrial strain will provide important value for the differentiation of these two.

LGE was present in 97.5% of RCM patients in our study groups. Patients with RCM, especially those with myocardial amyloidosis, often present with subendocardial LGE, patients with CP have less myocardial involvement, fewer abnormal enhancement changes in the myocardium, and the pericardium is mostly comprised of old fibers or calcifications without signs of enhancement. Despite the

presence of LGE findings in some patients with RCM, a substantial number do not exhibit significant evidence of this characteristic. Furthermore, the presence of LGE is not exclusive to RCM, as it can also be observed in other diseases such as cardiomyopathy and sarcoidosis. Therefore, LGE alone cannot serve as a diagnostic marker for RCM. Additionally, in cases where the use of contrast medium is contraindicated due to renal insufficiency or contrast allergy, non-enhanced myocardial strain analysis, particularly focusing on atrial strain, offers significant advantages in differentiating between these cardiac conditions. This study has some limitations. First, we included a small number of patients so that the prognostic value of atrial strain could not be evaluated, and in the future, more cases will be prospectively included to investigate the important value of atrial strain in the prognostic and efficacy evaluation of the study population. Second, because endocardial biopsy is difficult to perform clinically, this study is a retrospective one, so some patients with RCM lack the gold standard diagnosis of endocardial biopsy. We included endocardial enhancement and septal wall thickening on CMR in the diagnostic criteria for RCM, which could somewhat amplify the diagnostic value of LGE. However, our aim was to investigate the differential value of non-enhancing atrial myocardial strain parameters that reflect histological characteristics, and in the future, with the use of endocardial biopsy, the incremental predictive value of atrial strain will be explored compared with the remaining CMR parameters. Finally, similar to speckle tracking echocardiography technology [33], there are some differences in strain measurements between the CMR-FT technology post-processing software from different vendors. Further investigation of the applicability of other vendor software is therefore necessary to validate our findings.

5. Conclusion

In conclusion, CMR-FT derived assessment of left atrial strain is a useful method in the differential diagnosis of patients with CP and RCM. In particular, for patients with reduced LVEF, further analysis of LA-εs can help to differentiate CP from RCM, and this is especially useful in the patients with difficulty indifferentiating CP from RCM by extensive clinical and non-invasive tests.

Funding statement

This study was supported by grants from National Key R&D Program of China (2022YFE0209800), the National Natural Science Foundation of China (U1908211, 82271986), the Beijing Hospitals Authority Youth Programme, (code QML20230610).

Data availability statement

The data that support the findings of this study are available from the corresponding authors.

CRediT authorship contribution statement

Kairui Bo: Writing – original draft. **Yichen Zhao:** Methodology. **Xuelian Gao:** Formal analysis. **Yanchun Chen:** Visualization. **Yue Ren:** Data curation. **Yifeng Gao:** Methodology. **Zhen Zhou:** Supervision, Software. **Hui Wang:** Writing – original draft, Funding acquisition. **Lei Xu:** Validation, Funding acquisition.

Declaration of competing interest

We have reconfirmed that all authors have no conflicts of interest.

Acknowledgements

We would like to express my heartfelt gratitude to Professor Zhonghua Sun for his invaluable guidance and support throughout the course of this study.

References

[1] A. Aldajani, V. Mardigyan, M. Chetrit, A contemporary approach to the diagnosis and management of constrictive pericarditis, Can. J. Cardiol. 39 (2023) 1144–1148.
[2] M. Nahass, J. Kassotis, Constrictive pericarditis, N. Engl. J. Med. 389 (2023) 2087.
[3] C. Rapezzi, A. Aimo, A. Barison, M. Emdin, A. Porcari, A. Linhart, A. Keren, M. Merlo, G. Sinagra, Restrictive cardiomyopathy: definition and diagnosis, Eur. Heart J. 43 (2022) 4679–4693.
[4] J.W. Hirshfeld Jr., H. Johnston-Cox, Distinguishing constrictive pericarditis from restrictive cardiomyopathy-an ongoing diagnostic challenge, JAMA Cardiol. 7 (2022) 13–14.
[5] C.C. Jain, W.R. Miranda, A. El Sabbagh, R.A. Nishimura, A simplified method for the diagnosis of constrictive pericarditis in the cardiac catheterization laboratory, JAMA Cardiol. 7 (2022) 100–104.
[6] J.W. Lloyd, N.S. Anavekar, J.K. Oh, W.R. Miranda, Multimodality imaging in differentiating constrictive pericarditis from restrictive cardiomyopathy: a comprehensive overview for clinicians and imagers, J. Am. Soc. Echocardiogr. 36 (2023) 1254–1265.
[7] D.R. Talreja, W.D. Edwards, G.K. Danielson, H.V. Schaff, A.J. Tajik, H.D. Tazelaar, J.F. Breen, J.K. Oh, Constrictive pericarditis in 26 patients with histologically normal pericardial thickness, Circulation 108 (2003) 1852–1857.
[8] S. Liu, C. Ma, W. Ren, J. Yang, Y. Zhang, S. Li, Y. Cheng, Left atrial systolic and diastolic dysfunction in patients with chronic constrictive pericarditis: a study using speckle tracking and conventional echocardiography, PLoS One 8 (2013) e68718.
[9] S. Liu, C. Ma, W. Ren, J. Zhang, N. Li, J. Yang, Y. Zhang, W. Qiao, Regional left atrial function differentiation in patients with constrictive pericarditis and restrictive cardiomyopathy: a study using speckle tracking echocardiography, Int. J. Cardiovasc. Imag. 31 (2015) 1529–1536.

[10] R. Cau, P. Bassareo, J.S. Suri, G. Pontone, L. Saba, The emerging role of atrial strain assessed by cardiac MRI in different cardiovascular settings: an up-to-date review, Eur. Radiol. 32 (2022) 4384–4394.
[11] W. Yang, J. Xu, L. Zhu, Q. Zhang, Y. Wang, S. Zhao, M. Lu, Myocardial strain measurements derived from MR feature-tracking: influence of sex, age, field strength, and vendor, JACC Cardiovasc Imaging (2023). Online ahead of print.
[12] Z. Yang, H. Wang, S. Chang, J. Cui, L. Zhou, Q. Lv, Y. He, X. Du, J. Dong, C. Ma, Left ventricular strain-curve morphology to distinguish between constrictive pericarditis and restrictive cardiomyopathy, ESC Heart Fail 8 (2021) 4863–4872.
[13] T.D. Welch, L.H. Ling, R.E. Espinosa, N.S. Anavekar, H.J. Wiste, B.D. Lahr, H.V. Schaff, J.K. Oh, Echocardiographic diagnosis of constrictive pericarditis: mayo Clinic criteria, Circ. Cardiovasc. Imaging 7 (2014) 526–534.
[14] A.S. Antonopoulos, A. Vrettos, E. Androulakis, C. Kamperou, C. Vlachopoulos, K. Tsioufis, R. Mohiaddin, G. Lazaros, Cardiac magnetic resonance imaging of pericardial diseases: a comprehensive guide, Eur. Heart J. Cardiovasc. Imaging 8 (2023) 983–998.
[15] P.P. Sengupta, V.K. Krishnamoorthy, W.P. Abhayaratna, J. Korinek, M. Belohlavek, T.M. Sundt 3rd, K. Chandrasekaran, F. Mookadam, J.B. Seward, A.J. Tajik, B. K. Khandheria, Disparate patterns of left ventricular mechanics differentiate constrictive pericarditis from restrictive cardiomyopathy, JACC Cardiovasc Imaging 1 (2008) 29–38.
[16] C.M. Kramer, J. Barkhausen, C. Bucciarelli-Ducci, S.D. Flamm, R.J. Kim, E. Nagel, Standardized cardiovascular magnetic resonance imaging (CMR) protocols: 2020 update, J. Cardiovasc. Magn. Reson. 22 (2020) 17.
[17] J.T. Kowallick, S. Kutty, F. Edelmann, A. Chiribiri, A. Villa, M. Steinmetz, J.M. Sohns, W. Staab, N. Bettencourt, C. Unterberg-Buchwald, G. Hasenfuß, J. Lotz, A. Schuster, Quantification of left atrial strain and strain rate using Cardiovascular Magnetic Resonance myocardial feature tracking: a feasibility study, J. Cardiovasc. Magn. Reson. 16 (2014) 60.
[18] A. Bernardini, A. Camporeale, M. Pieroni, F. Pieruzzi, S. Figliozzi, P. Lusardi, M. Spada, R. Mignani, A. Burlina, F. Carubbi, Y. Battaglia, F. Graziani, S. Pica, L. Tondi, K. Chow, S. Boveri, I. Olivotto, M. Lombardi, Atrial dysfunction assessed by cardiac magnetic resonance as an early marker of fabry cardiomyopathy, JACC Cardiovasc Imaging 13 (2020) 2262–2264.
[19] B. Raman, R.W. Smillie, M. Mahmod, K. Chan, R. Ariga, C. Nikolaidou, E. Ormondroyd, K. Thomson, A.R. Harper, G. Tan, A.J. Lewandowski, F. Rodriguez Bajo, E.C. Wicks, B. Casadei, H. Watkins, S. Neubauer, Incremental value of left atrial booster and reservoir strain in predicting atrial fibrillation in patients with hypertrophic cardiomyopathy: a cardiovascular magnetic resonance study, J. Cardiovasc. Magn. Reson. 23 (2021) 109.
[20] H. Wang, K. Bo, Y. Gao, Z. Zhou, X. Gao, Z. Sun, L. Xu, Cardiac magnetic resonance analysis of left atrium function in patients with pre-apical hypertrophic cardiomyopathy, Quant. Imag. Med. Surg. 14 (2023) 888–897.
[21] F. Yang, L. Wang, J. Wang, L. Pu, Y. Xu, W. Li, K. Wan, D. Yang, J. Sun, Y. Han, Y. Zhu, Y. Chen, Prognostic value of fast semi-automated left atrial long-axis strain analysis in hypertrophic cardiomyopathy, J. Cardiovasc. Magn. Reson. 23 (2021) 36.
[22] L. Hopman, M.J. Mulder, A.M. van der Laan, A. Demirkiran, P. Bhagirath, A.C. van Rossum, C.P. Allaart, M.J.W. Götte, Impaired left atrial reservoir and conduit strain in patients with atrial fibrillation and extensive left atrial fibrosis, J. Cardiovasc. Magn. Reson. 23 (2021) 131.
[23] V.T. Truong, C. Palmer, M. Young, S. Wolking, T.N.M. Ngo, B. Sheets, C. Hausfeld, A. Ornella, M.D. Taylor, K.M. Zareba, S.V. Raman, W. Mazur, Right atrial deformation using cardiovascular magnetic resonance myocardial feature tracking compared with two-dimensional speckle tracking echocardiography in healthy volunteers, Sci. Rep. 10 (2020) 5237.
[24] V.T. Truong, C. Palmer, S. Wolking, B. Sheets, M. Young, T.N.M. Ngo, M. Taylor, S.F. Nagueh, K.M. Zareba, S. Raman, W. Mazur, Normal left atrial strain and strain rate using cardiac magnetic resonance feature tracking in healthy volunteers, Eur. Heart J. Cardiovasc. Imaging 21 (2020) 446–453.
[25] K. Nochioka, C.C. Quarta, B. Claggett, G.Q. Roca, C. Rapezzi, R.H. Falk, S.D. Solomon, Left atrial structure and function in cardiac amyloidosis, Eur. Heart J. Cardiovasc. Imaging 18 (2017) 1128–1137.
[26] S. Ichimata, Y. Hata, K. Hirono, Y. Yamaguchi, N. Nishida, Clinicopathological features of clinically undiagnosed sporadic transthyretin cardiac amyloidosis: a forensic autopsy-based series, Amyloid 28 (2021) 125–133.
[27] C.C. Singulane, J.A. Slivnick, K. Addetia, F.M. Asch, N. Sarswat, L. Soulat-Dufour, V. Mor-Avi, R.M. Lang, Prevalence of right atrial impairment and association with outcomes in cardiac amyloidosis, J. Am. Soc. Echocardiogr. 35 (2022) 829–835.e1.
[28] H. Cheng, S. Zhao, S. Jiang, M. Lu, C. Yan, J. Ling, Y. Zhang, Q. Liu, N. Ma, G. Yin, R. Jerecic, Z. He, The relative atrial volume ratio and late gadolinium enhancement provide additive information to differentiate constrictive pericarditis from restrictive cardiomyopathy, J. Cardiovasc. Magn. Reson. 13 (2011) 15.
[29] R. Soler, E. Rodríguez, C. Remuiñán, M.J. Bello, A. Díaz, Magnetic resonance imaging of primary cardiomyopathies, J. Comput. Assist. Tomogr. 27 (2003) 724–734.
[30] F. Bandera, R. Martone, L. Chacko, S. Ganesananthan, J.A. Gilbertson, M. Ponticos, T. Lane, A. Martinez-Naharro, C. Whelan, C. Quarta, D. Rowczenio, R. Patel, Y. Razvi, H. Lachmann, A. Wechelakar, J. Brown, D. Knight, J. Moon, A. Petrie, F. Cappelli, M. Guazzi, L. Potena, C. Rapezzi, O. Leone, P.N. Hawkins, J. D. Gillmore, M. Fontana, Clinical importance of left atrial infiltration in cardiac transthyretin amyloidosis, JACC Cardiovasc Imaging 15 (2022) 17–29.
[31] A. Brand, D. Frumkin, A. Hübscher, H. Dreger, K. Stangl, G. Baldenhofer, F. Knebel, Phasic left atrial strain analysis to discriminate cardiac amyloidosis in patients with unclear thick heart pathology, Eur. Heart J. Cardiovasc. Imaging 22 (2021) 680–687.
[32] M. Amaki, J. Savino, D.L. Ain, J. Sanz, G. Pedrizzetti, H. Kulkarni, J. Narula, P.P. Sengupta, Diagnostic concordance of echocardiography and cardiac magnetic resonance-based tissue tracking for differentiating constrictive pericarditis from restrictive cardiomyopathy, Circ. Cardiovasc. Imaging 7 (2014) 819–827.
[33] G. Pedrizzetti, P. Claus, P.J. Kilner, E. Nagel, Principles of cardiovascular magnetic resonance feature tracking and echocardiographic speckle tracking for informed clinical use, J. Cardiovasc. Magn. Reson. 18 (2016) 51.